Optimization of ride comfort for a three-axle vehicle equipped with interconnected hydro-pneumatic suspension system

Ferhat Saglam[*1] and Y. Samim Unlusoy[2a]

[1]*ASELSAN Incorporation, Ankara, Turkey*
[2]*Middle East Technical University, Mechanical Engineering Department, Ankara, Turkey*

Abstract. The aim of this study is the optimization of the parameters of interconnected Hydro-Pneumatic (HP) suspension system of a three-axle vehicle for ride comfort and handling. For HP suspension systems of equivalent vertical stiffness and damping characteristics, interconnected HP suspension systems increase roll and pitch stiffness and damping characteristics of the vehicle as compared to unconnected HP suspension systems. Thus, they result in improved handling and braking/acceleration performances of the vehicle. However, increased roll and pitch stiffness and damping characteristics also increase roll and pitch accelerations, which in turn result in degraded ride comfort performance. Therefore, in order to improve both ride comfort and vehicle handling performances simultaneously, an optimum parameter set of an interconnected HP suspension system is obtained through an optimization procedure. The objective function is formed as the sum of the weighted vertical accelerations according to ISO 2631. The roll angle, one of the important measures of vehicle handling and driving safety, is imposed as a constraint in the optimization study. Upper and lower parameter bounds are used in the optimization in order to get a physically realizable parameter set. Optimization procedure is implemented for a three-axle vehicle with unconnected and interconnected suspension systems separately. Optimization results show that interconnected HP suspension system results in improvements in both ride comfort and vehicle handling performance, as compared to the unconnected suspension system. As a result, interconnected HP suspension systems present a solution to the conflict between ride comfort and vehicle handling which is present in unconnected suspension systems.

Keywords: hydro-pneumatic suspension; interconnected suspension; ride comfort; vehicle handling; optimization; roll angle; three-axle vehicle

1. Introduction

In this study, optimization of the suspension parameters for a three-axle vehicle equipped with Hydro-Pneumatic (HP) suspension system for ride for comfort and handling is performed. As Fig. 1 shows, in its basic structure, HP suspension system consists of a gas volume, two oil volumes, floating piston, main piston, hydraulic cylinder and an orifice or damper valve. The gas volume provides HP suspension system with elasticity and flow of oil through the orifice or damper valve
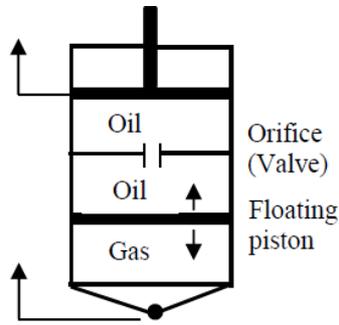

Fig. 1 HP suspension model

with damping characteristics.

HP suspension systems have certain advantages with respect to conventional mechanical suspension systems, Bauer (2011). One of the most significant advantages of the HP suspension system is that active and semi-active suspension applications can be easily incorporated. Another important advantage of the HP suspension systems as compared to mechanical suspension systems is that on a vehicle, HP suspension units (left/right/front/intermediate/rear) can be conveniently interconnected to each other by using hydraulic conductors with relative ease. By these interconnections, a response created in one suspension unit by the inputs originated from the vehicle body or from tire/road interaction can be transmitted to other suspension units. Thus, interactions and communications among different suspension units can be performed, and it is possible to improve certain performance characteristics of the vehicle. In contrast, with mechanical suspension systems interconnections among suspension units are more difficult and impractical especially in the pitch direction.

In case of vehicles with passive suspension systems, there is a conflict between ride comfort and handling. A relatively soft suspension setting is required for good ride comfort and a somewhat stiff suspension setting improves vehicle handling. Thus, it is not possible to improve both of the suspension performance measures simultaneously. One of the possible solutions for improving vehicle handling and ride comfort simultaneously is the use of active or semi-active suspension systems. Another possible solution is the use of interconnected suspension systems.

In literature, one can find a number of recent studies on the interconnected HP suspension systems and hydraulically interconnected suspension systems. In the study by Saglam and Unlusoy (2016a), modelling and simulation of a three-axle vehicle with interconnected HP suspension system was studied. A full vehicle model with an interconnected HP suspension system in coupled roll and pitch directions was modelled, and then the performance evaluations of the designed interconnected system for ride comfort and vehicle handling were performed by simulations. In the study of Cao (2008), a HP suspension system was modelled and then roll, pitch, and coupled roll and pitch interconnections for a two-axle vehicle were studied. Further, the effects of the interconnections on vehicle ride comfort, handling, and braking/acceleration performance were also analysed. Zhang *et al.* (2010a, b) studied the frequency dependent model of a hydraulically interconnected mechanical suspension system in the pitch plane. In order to evaluate ride comfort performance of the interconnected suspension system, a test setup was prepared and tests were performed. Results from the model and experiments were compared and the interconnected suspension model was validated. Zhang *et al.* (2011) developed a full vehicle model with hydraulically interconnected suspension system. According to vehicle handling simulations,

hydraulically interconnected suspension systems improved vehicle handling, yet they reduced vehicle ride comfort for a two-axle vehicle. Ding *et al.* (2012) studied the modelling of a three-axle vehicle with hydraulically interconnected mechanical suspension system in the pitch plane. The results showed that hydraulically interconnected suspension system improves the pitch motion without sacrificing ride comfort performance. Another potential use of the interconnected HP suspension system is to equalize or distribute the load among the axle group of heavy commercial vehicle. In the study of the Saglam and Unlusoy (2016b), an interconnected HP suspension system was studied for the rear axle group of a heavy commercial vehicle for load sharing purposes. Static and dynamic load sharing performance of the designed interconnected HP suspension system was examined by the simulations.

In the studies mentioned so far, the aim is the modelling and simulation of the vehicle with interconnected HP suspension system, and nominal parameter sets are used in simulations. In literature, there are also studies related to the optimization of the unconnected HP suspension system. Thoresson (2003) studied the optimization of the suspension system parameters of a two-axle off-road vehicle for ride comfort and handling. The parameters, damping characteristics scale coefficients, and the HP suspension gas volumes of the front and rear suspensions are optimized. Objection function for the vehicle ride comfort and handling was defined as the weighted root mean square (rms) of the vertical acceleration and body roll angle, respectively. Thoresson *et al.* (2009a, b) studied the modelling of a simplified vehicle ride and vehicle handling to be used in the vehicle suspension optimization and the full vehicle model in MSC ADAMS software. The simplified vehicle models were used for the gradient information and the full vehicle model was used for the objective function evaluation. Normalized HP suspension gas volumes and normalized damper scale factors were again used as the parameters to be optimized. Optimization was performed according to ride comfort, handling, and both ride comfort and handling. As expected, for handling optimization, gas volumes were set to the lower boundary values and damping values were set to upper boundary values. For ride comfort, gas volumes were set to upper boundary values and damping values were set to lower boundary values. For combined ride comfort and handling optimization, the damping values and gas volumes were set to values within the parameter space for compromised solution. Els and Uys (2003) studied the optimization of a HP suspension system for ride comfort and handling. Parameters of the suspension system, HP suspension gas volumes and damping scale factors, were optimized. The cost function to be minimized was formed as the weighted rms of the vertical acceleration in the Belgian paved road simulation, and the optimization constraint was formed as the maximum roll angle in the lane change simulation. Then, maximum roll angle was taken as the cost function and rms of the vertical acceleration was used as the optimization constraint. As the conclusion of the study, it was suggested that optimization should be performed for improved handling for better optimization results.

The literature survey shows the existence of studies on the optimization of unconnected HP suspension systems for ride comfort and vehicle handling. It is noted, however, that there is no published study related to the optimization of interconnected suspension system parameters of multi-axle vehicles for simultaneous ride comfort and vehicle handling. For unconnected suspension systems, the optimization results show that there is a compromise solution for ride comfort and vehicle handling. However, as will be explored in the following sections, by using the potential performance of the interconnected HP suspension system, it is possible to improve vehicle ride comfort and handling performances simultaneously.

In the following sections, modelling of the interconnected HP suspension system for a full

vehicle model, and modelling of a full vehicle are going to be detailed. Then optimization of the parameters of the interconnected HP suspension system for ride comfort and vehicle handling will be performed, and the optimization results are illustrated. Optimization is performed for both interconnected and unconnected HP suspension systems. The performance of the interconnected system is assessed taking the performance of the unconnected HP suspension as the reference. Finally, the results obtained in this study are discussed and conclusions are presented.

2. Modelling of the interconnected HP suspension system

Modelling and simulation of the HP suspension systems have been performed in a number of studies, Saglam and Unlusoy (2014), Joo (1991), Cao (2008), Saglam (2016). In this study, a three-axle vehicle with interconnected HP suspension system in coupled roll and pitch is modelled and used in simulations. The interconnection of the HP suspension system is configured for increasing roll and pitch stiffness and damping as shown in Fig. 2, Saglam and Unlusoy (2016a).
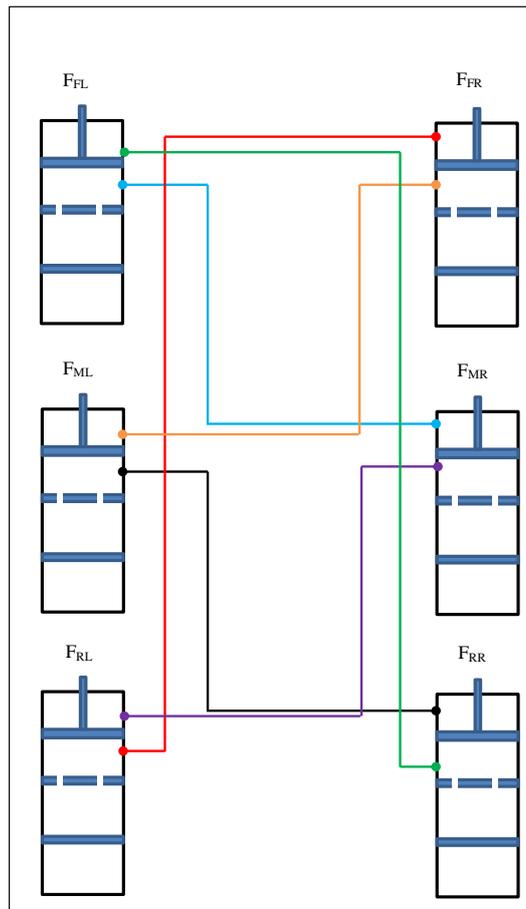

Fig. 2 Interconnected HP suspension system in coupled roll and pitch direction for a three-axle vehicle

As Fig. 2 illustrates, all suspension units are interconnected to each other in the lateral and longitudinal directions by hydraulic conductors. Front left, front right, intermediate left, intermediate right, rear left, and rear right suspension forces are given as, Saglam (2016),

$$
\begin{aligned}
F_{FL} = &\frac{P_{30FL} V_{30FL}^{\kappa} A_p}{\left[V_{30FL} + A_p \left(z_{pFL} - z_{tFL} - \frac{A_{pr}}{A_p} \left(z_{pMR} - z_{tMR} \right) \right) \right]^{\kappa}} - \\
&-\frac{P_{30RR} V_{30RR}^{\kappa} A_{pr}}{\left[V_{30RR} + A_p \left(z_{pRR} - z_{tRR} - \frac{A_{pr}}{A_p} \left(z_{pFL} - z_{tFL} \right) \right) \right]^{\kappa}} - \\
&-A_p \left[\frac{A_p \left(\dot{z}_{pFL} - \dot{z}_{tFL} \right) - A_{pr} \left(\dot{z}_{pMR} - \dot{z}_{tMR} \right)}{A_v C_D} \right]^2 \frac{\rho}{2} \operatorname{sign} \left[\begin{array}{l} A_p \left(\dot{z}_{pFL} - \dot{z}_{tFL} \right) - \\ -A_{pr} \left(\dot{z}_{pMR} - \dot{z}_{tMR} \right) \end{array} \right] + \\
&+A_{pr} \left[\frac{A_p \left(\dot{z}_{pRR} - \dot{z}_{tRR} \right) - A_{pr} \left(\dot{z}_{pFL} - \dot{z}_{tFL} \right)}{A_v C_D} \right]^2 \frac{\rho}{2} \operatorname{sign} \left[\begin{array}{l} A_p \left(\dot{z}_{pRR} - \dot{z}_{tRR} \right) - \\ -A_{pr} \left(\dot{z}_{pFL} - \dot{z}_{tFL} \right) \end{array} \right] - \\
&-\frac{A_{pr}^2 \left(\dot{z}_{pFL} - \dot{z}_{tFL} \right)}{R_{4FL1RR}}
\end{aligned}
\tag{1}
$$

$$
\begin{aligned}
F_{FR} = &\frac{P_{30FR} V_{30FR}^{\kappa} A_p}{\left[V_{30FR} + A_p \left(z_{pFR} - z_{tFR} - \frac{A_{pr}}{A_p} \left(z_{pML} - z_{tML} \right) \right) \right]^{\kappa}} - \\
&-\frac{P_{30RL} V_{30RL}^{\kappa} A_{pr}}{\left[V_{30RL} + A_p \left(z_{pRL} - z_{tRL} - \frac{A_{pr}}{A_p} \left(z_{pFR} - z_{tFR} \right) \right) \right]^{\kappa}} - \\
&-A_p \left[\frac{A_p \left(\dot{z}_{pFR} - \dot{z}_{tFR} \right) - A_{pr} \left(\dot{z}_{pML} - \dot{z}_{tML} \right)}{A_v C_D} \right]^2 \frac{\rho}{2} \operatorname{sign} \left[\begin{array}{l} A_p \left(\dot{z}_{pFR} - \dot{z}_{tFR} \right) - \\ -A_{pr} \left(\dot{z}_{pML} - \dot{z}_{tML} \right) \end{array} \right] + \\
&+A_{pr} \left[\frac{A_p \left(\dot{z}_{pRL} - \dot{z}_{tRL} \right) - A_{pr} \left(\dot{z}_{pFR} - \dot{z}_{tFR} \right)}{A_v C_D} \right]^2 \frac{\rho}{2} \operatorname{sign} \left[\begin{array}{l} A_p \left(\dot{z}_{pRL} - \dot{z}_{tRL} \right) - \\ -A_{pr} \left(\dot{z}_{pFR} - \dot{z}_{tFR} \right) \end{array} \right] - \\
&-\frac{A_{pr}^2 \left(\dot{z}_{pFR} - \dot{z}_{tFR} \right)}{R_{4FR1RL}}
\end{aligned}
\tag{2}
$$

$$
\begin{aligned}
F_{ML} = &\frac{P_{30ML} V_{30ML}^{\kappa} A_p}{\left[V_{30ML} + A_p \left(z_{pML} - z_{tML} - \frac{A_{pr}}{A_p} \left(z_{pRR} - z_{tRR} \right) \right) \right]^{\kappa}} - \\
&-\frac{P_{30FR} V_{30FR}^{\kappa} A_{pr}}{\left[V_{30FR} + A_p \left(z_{pFR} - z_{tFR} - \frac{A_{pr}}{A_p} \left(z_{pML} - z_{tML} \right) \right) \right]^{\kappa}} - \\
&-A_p \left[\frac{A_p \left(\dot{z}_{pML} - \dot{z}_{tML} \right) - A_{pr} \left(\dot{z}_{pRR} - \dot{z}_{tRR} \right)}{A_v C_D} \right]^2 \frac{\rho}{2} \operatorname{sign} \left[\begin{array}{l} A_p \left(\dot{z}_{pML} - \dot{z}_{tML} \right) - \\ -A_{pr} \left(\dot{z}_{pRR} - \dot{z}_{tRR} \right) \end{array} \right] + \\
&+A_{pr} \left[\frac{A_p \left(\dot{z}_{pFR} - \dot{z}_{tFR} \right) - A_{pr} \left(\dot{z}_{pML} - \dot{z}_{tML} \right)}{A_v C_D} \right]^2 \frac{\rho}{2} \operatorname{sign} \left[\begin{array}{l} A_p \left(\dot{z}_{pFR} - \dot{z}_{tFR} \right) - \\ -A_{pr} \left(\dot{z}_{pML} - \dot{z}_{tML} \right) \end{array} \right] - \\
&-\frac{A_{pr}^2 \left(\dot{z}_{pML} - \dot{z}_{tML} \right)}{R_{4ML1FR}}
\end{aligned}
\tag{3}
$$

$$F_{MR} = \frac{P_{30MR} V_{30MR}^{\kappa} A_p}{\left[V_{30MR} + A_p \left(z_{pMR} - z_{tMR} - \frac{A_{pr}}{A_p} \left(z_{pRL} - z_{tRL} \right) \right) \right]^{\kappa}} -$$

$$- \frac{P_{30FL} V_{30FL}^{\kappa} A_{pr}}{\left[V_{30FL} + A_p \left(z_{pFL} - z_{tFL} - \frac{A_{pr}}{A_p} \left(z_{pMR} - z_{tMR} \right) \right) \right]^{\kappa}} -$$

$$- A_p \left[\frac{A_p \left(\dot{z}_{pMR} - \dot{z}_{tMR} \right) - A_{pr} \left(\dot{z}_{pRL} - \dot{z}_{tRL} \right)}{A_v C_D} \right]^2 \frac{\rho}{2} \mathrm{sign} \left[\begin{array}{c} A_p \left(\dot{z}_{pMR} - \dot{z}_{tMR} \right) - \\ - A_{pr} \left(\dot{z}_{pRL} - \dot{z}_{tRL} \right) \end{array} \right] +$$

$$+ A_{pr} \left[\frac{A_p \left(\dot{z}_{pFL} - \dot{z}_{tFL} \right) - A_{pr} \left(\dot{z}_{pMR} - \dot{z}_{tMR} \right)}{A_v C_D} \right]^2 \frac{\rho}{2} \mathrm{sign} \left[\begin{array}{c} A_p \left(\dot{z}_{pFL} - \dot{z}_{tFL} \right) - \\ - A_{pr} \left(\dot{z}_{pMR} - \dot{z}_{tMR} \right) \end{array} \right] -$$

$$- \frac{A_{pr}^2 \left(\dot{z}_{pMR} - \dot{z}_{tMR} \right)}{R_{4MR1FL}}$$

$$(4)$$

$$F_{RL} = \frac{P_{30RL} V_{30RL}^{\kappa} A_p}{\left[V_{30RL} + A_p \left(z_{pRL} - z_{tRL} - \frac{A_{pr}}{A_p} \left(z_{pFR} - z_{tFR} \right) \right) \right]^{\kappa}} -$$

$$- \frac{P_{30MR} V_{30MR}^{\kappa} A_{pr}}{\left[V_{30MR} + A_p \left(z_{pMR} - z_{tMR} - \frac{A_{pr}}{A_p} \left(z_{pRL} - z_{tRL} \right) \right) \right]^{\kappa}} -$$

$$- A_p \left[\frac{A_p \left(\dot{z}_{pRL} - \dot{z}_{tRL} \right) - A_{pr} \left(\dot{z}_{pFR} - \dot{z}_{tFR} \right)}{A_v C_D} \right]^2 \frac{\rho}{2} \mathrm{sign} \left[\begin{array}{c} A_p \left(\dot{z}_{pRL} - \dot{z}_{tRL} \right) - \\ - A_{pr} \left(\dot{z}_{pFR} - \dot{z}_{tFR} \right) \end{array} \right] +$$

$$+ A_{pr} \left[\frac{A_p \left(\dot{z}_{pMR} - \dot{z}_{tMR} \right) - A_{pr} \left(\dot{z}_{pRL} - \dot{z}_{tRL} \right)}{A_v C_D} \right]^2 \frac{\rho}{2} \mathrm{sign} \left[\begin{array}{c} A_p \left(\dot{z}_{pMR} - \dot{z}_{tMR} \right) - \\ - A_{pr} \left(\dot{z}_{pRL} - \dot{z}_{tRL} \right) \end{array} \right] -$$

$$- \frac{A_{pr}^2 \left(\dot{z}_{pRL} - \dot{z}_{tRL} \right)}{R_{4RL1MR}}$$

$$(5)$$

$$F_{RR} = \frac{P_{30RR} V_{30RR}^{\kappa} A_p}{\left[V_{30RR} + A_p \left(z_{pRR} - z_{tRR} - \frac{A_{pr}}{A_p} \left(z_{pFL} - z_{tFL} \right) \right) \right]^{\kappa}} -$$

$$- \frac{P_{30ML} V_{30ML}^{\kappa} A_{pr}}{\left[V_{30ML} + A_p \left(z_{pML} - z_{tML} - \frac{A_{pr}}{A_p} \left(z_{pRR} - z_{tRR} \right) \right) \right]^{\kappa}} -$$

$$- A_p \left[\frac{A_p \left(\dot{z}_{pRR} - \dot{z}_{tRR} \right) - A_{pr} \left(\dot{z}_{pFL} - \dot{z}_{tFL} \right)}{A_v C_D} \right]^2 \frac{\rho}{2} \mathrm{sign} \left[\begin{array}{c} A_p \left(\dot{z}_{pRR} - \dot{z}_{tRR} \right) - \\ - A_{pr} \left(\dot{z}_{pFL} - \dot{z}_{tFL} \right) \end{array} \right] +$$

$$+ A_{pr} \left[\frac{A_p \left(\dot{z}_{pML} - \dot{z}_{tML} \right) - A_{pr} \left(\dot{z}_{pRR} - \dot{z}_{tRR} \right)}{A_v C_D} \right]^2 \frac{\rho}{2} \mathrm{sign} \left[\begin{array}{c} A_p \left(\dot{z}_{pML} - \dot{z}_{tML} \right) - \\ - A_{pr} \left(\dot{z}_{pRR} - \dot{z}_{tRR} \right) \end{array} \right] -$$

$$- \frac{A_{pr}^2 \left(\dot{z}_{pRR} - \dot{z}_{tRR} \right)}{R_{4RR1ML}}$$
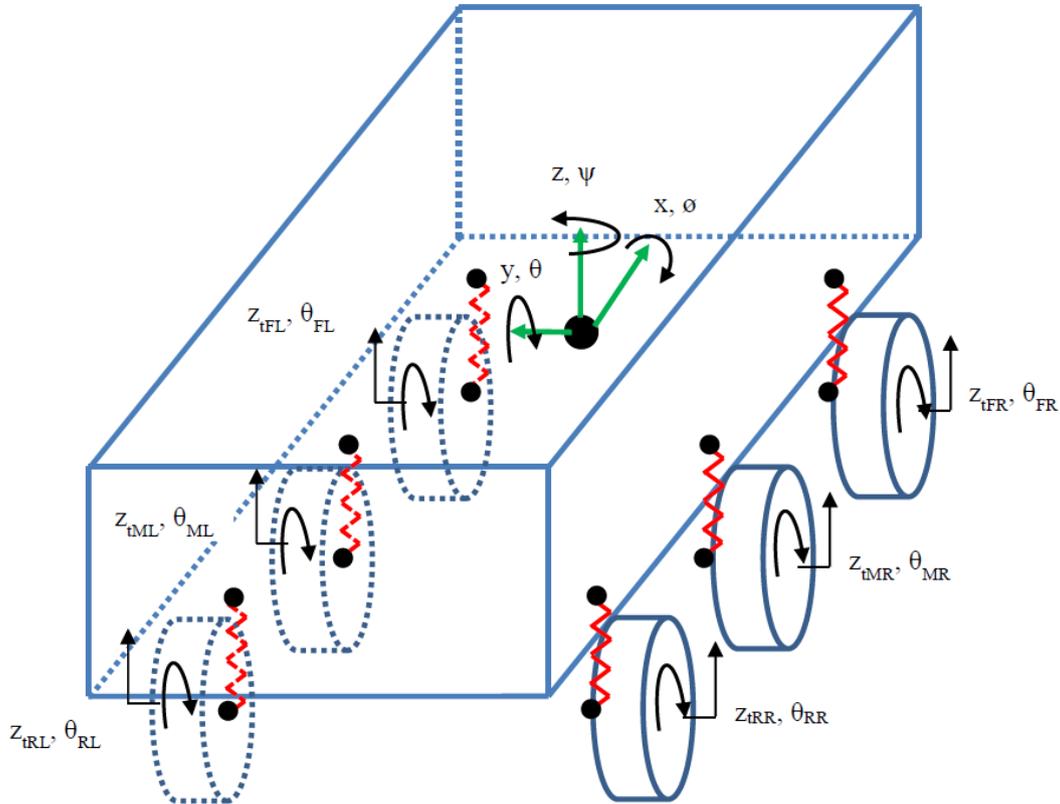
$$(6)$$

Fig. 3 Eighteen degree of freedom full vehicle model, Saglam and Unlusoy (2016a)

In these equations P_{30}'s are the initial gas pressures at static equilibrium, V_{30}'s are the initial gas volumes at static equilibrium, κ is the polytropic gas constant, z_p's are the piston displacement, z_t's are the tire displacement, A_p is the piston area, A_{pr} is the difference between the piston and piston rod area, A_v is the orifice opening area, C_D is the orifice damping loss factor, ρ is the oil density, and R_{41}'s are the hydraulic conductor resistance, and "FL", "FR", "ML", "MR", "RL", and "RR" stand for the front left, front right, intermediate left, intermediate right, rear left, and rear right, respectively.

The important characteristics of the interconnected suspension system is its ability to increase roll and pitch stiffness and damping characteristics without increasing the vertical stiffness and damping characteristics. For a vehicle with unconnected HP suspension configuration, the only way of increasing the roll and pitch stiffness and damping characteristics is to increase vertical stiffness and damping characteristic. In the study by Saglam and Unlusoy (2016a), roll and pitch stiffness and damping characteristics of the vehicles with unconnected and interconnected HP suspension systems were compared. It was concluded that when the vertical stiffness and damping characteristics of the vehicle with unconnected and interconnected HP suspension systems are equalized to each other, the vehicle with interconnected HP suspension system has higher roll and pitch stiffness and damping characteristics.

Interconnected HP suspension system is incorporated into the eighteen degree of freedom full vehicle model shown in Fig. 3, Saglam and Unlusoy (2016a). Full vehicle model consists of
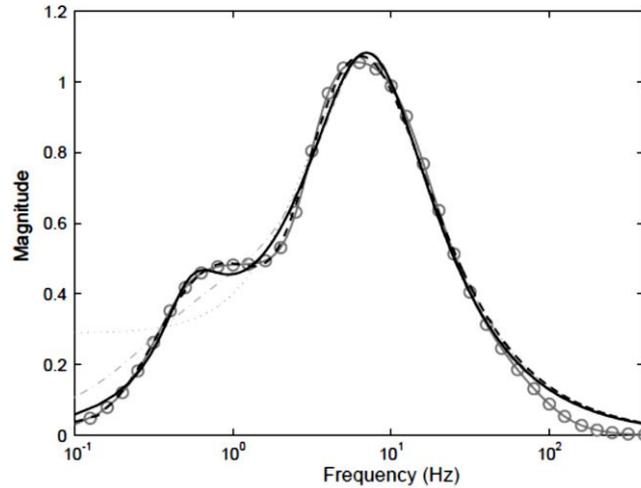
Fig. 4 Weighting frequency approximation of the ISO-2631 weighting curve for vertical acceleration, Zuo and Nayfeh (2003)

lateral, longitudinal, vertical, roll, pitch, and yaw degrees of freedom of the sprung mass, and rotational and vertical degrees of freedom of the six wheels with a total of eighteen degree of freedom. Magic Formula tire model with combined lateral and longitudinal tire forces is integrated into the full vehicle model, Saglam (2016).

3. Optimization of the parameters of the interconnected HP suspension system for ride comfort

The main aims of the suspension system are to isolate the vehicle from disturbances coming from the tire/road interaction, to keep the tires in contact with the road, and to guarantee vehicle driving safety. Due to the conflict between the ride comfort and vehicle handling performances, a conventional unconnected suspension system cannot improve these performance characteristics simultaneously. A search for improved vehicle handling ends up with increased vertical suspension stiffness and damping to increase roll and pitch stiffness and damping characteristics of the vehicle. This improvement in vehicle handling, however, is accompanied with reduced ride comfort for a vehicle with unconnected suspension system. Therefore, optimum suspension characteristics are decided with a compromise set of parameter values for acceptable ride comfort and vehicle handling performances. In order to satisfy these conflicting performance requirements, active and semi-active suspension systems with considerable additional complexity and cost may be utilized. Here, the use of interconnected suspension systems is presented as an alternative solution.

Vehicle ride comfort performance, in general, is evaluated with the vehicle vertical acceleration. The international standard ISO 2631 (1977) "Guide for the Evaluation of Human Exposure to Whole-Body Vibrations" has been commonly used for the evaluation of ride comfort. This standard provides a quantitative procedure for the evaluation of human exposure to vehicle accelerations for vertical and plane vibrations. Human sensitivity to vibration changes with

vibration amplitude, direction, duration, and frequency content. According to the ISO 2631 standard, human exposure to vibrations can be evaluated in a quantitative manner by the so called reduced comfort boundaries. These reduced comfort boundaries provide the rms values of the limiting acceleration values in different directions for different exposure durations, and in a range of frequencies. Frequency shaping filters are commonly used to evaluate the results of vibration exposure. In the study by Zuo and Nayfeh (2003), low-order continuous time filter for the ride comfort frequency weighting curves given in Fig. 3 is obtained.

The third order mathematical representation of this filter shown is given as, (Zuo and Nayfeh 2003)

$$W_k(s) = \frac{80.03s^2 + 989.0s + 0.02108}{s^3 + 78.92s^2 + 2412s + 5614} \tag{7}$$

For the interconnected HP suspension system, the design parameters are initial gas volumes at static equilibrium, piston areas, orifice or damper valve parameters, and for the interconnected suspension system the piston rod areas. Among these parameters, piston and piston rod areas affect both suspension stiffness and damping. On the other hand, gas volumes only affect suspension stiffness, and orifice or valve parameters only affect suspension damping. By changing the piston area, oil and gas pressures can be tuned to physically realizable values. In order to simplify the optimization study, piston rod area is not included in optimized parameter set. The design parameters of the interconnected and unconnected HP suspension systems and the related suspension characteristics of the design parameters are summarized in Table 1.

Table 1 Design and optimized suspension parameters

	Suspension Design Parameters	Optimized Parameters
Stiffness	A_p, A_r, V_{30}	A_r, V_{30}
Damping	A_p, A_r, Orifice or Valve Parameters	A_r, Orifice or Valve Parameters

In optimization, instead of using these parameters directly, their normalized values are used. These normalized parameters are defined as,

$$n_{V30} = \frac{V_{30n}}{V_{30}} \tag{8}$$

$$n_{Damp} = \frac{c_n}{c} \tag{9}$$

$$n_{Ar} = \frac{A_{rn}}{A_p} \tag{10}$$

In these equations, n_{v30} represents the normalized gas volume, V_{30n} represents nominal gas volume, n_{Damp} represents normalized valve or orifice damping, c_n represents nominal valve or orifice characteristics, c represents valve or orifice damping, n_{Ar} represents normalized piston rod area, A_{rn} represents nominal piston rod area, and A_p represents piston area. In order to get
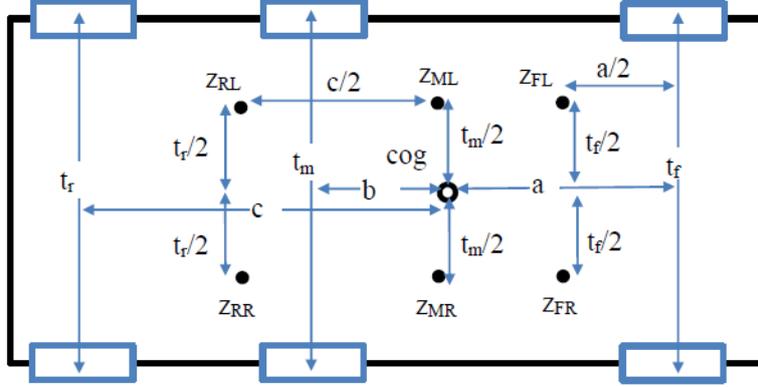
Fig. 5 Sprung mass vertical acceleration position

realizable physical parameter sets in optimization, lower and upper parameter constraints were defined as

$$n_{V30} \in \{0.4, 2.5\}$$

$$n_{Damp} \in \{0.4, 2.5\}$$

$$n_{Ar} \in \{0.6, 1\}$$

When n_{Ar} is equal to one, the piston and piston rod areas become equal, then the suspension is mathematically unconnected. On the other hand, when n_{Ar} is lower than one, the suspension becomes interconnected. In case of the interconnected HP suspension system, when n_{Ar} is further decreased, the amount of oil displaced between different suspension units increase, and the strength of the interconnected HP suspension system increases. Thus, this parameter may be used as a measure of the level or strength of interconnection. For example, when the piston rod area is decreased, the level of interconnection for the suspension system is emphasized. On the other hand, when the piston rod area is increased, the suspension characteristics get closer to those of unconnected configuration.

Since the ride comfort is related to the vertical, roll, and pitch accelerations, the objective function is formed by the weighted summation of the vertical, roll, and the pitch accelerations of the sprung mass. On the other hand, roll angle response is one of the most significant measures of vehicle handling and driving safety, Els and Uys (2003). In order to improve vehicle handling performance, roll angle of the vehicle should be reduced as much as possible. A vehicle with higher roll stiffness and damping characteristics has the low roll angle response during specified manoeuvre and thus provides better handling behaviour. Thus, to be able to take handling and driving safety into consideration, a constraint on the roll angle is imposed. Here, the optimization problem is defined in the standard form

$$\arg\min_{n_{V30}, n_{Damp}, n_{Ar}} \left\{ W_k(f) \left[\ddot{z}_{FL} + \ddot{z}_{FR} + \ddot{z}_{ML} + \ddot{z}_{MR} + \ddot{z}_{RL} + \ddot{z}_{RR} \right] \right\}$$

subject to

$$n_{V30} \in \{ n_{V30\,min}, n_{V30\,max} \}$$

$$n_{Damp} \in \{ n_{Damp\,min}, n_{Damp\,max} \}$$

$$n_{Ar} \in \{ n_{Ar\,min}, n_{Ar\,max} \}$$

$$\phi < \phi_{max}$$

In these equations $W_k(k)$ is frequency filter which is given in Fig. 4 and, z_{FL}, z_{FR}, z_{ML}, z_{MR}, z_{RL}, z_{RR} are the vertical displacements of the sprung mass at different locations shown in Fig. 5 and ϕ is the roll angle. The positions of the vertical acceleration points are chosen as to represent the positions of the seats in the vehicle.

Before the optimization study, in order to see the effects of the optimized parameters on the vertical acceleration and the roll angle, a parametric study is conducted and then the optimization study is performed. For ride comfort evaluations, simulations are performed with random road displacement input. Power spectral densities of the random road displacement input at different forward speeds are given in Fig. 6. Similarly, lane change simulations are performed for the handling performance evaluations. Steering input for the lane change manoeuvre is shown in Fig. 7.
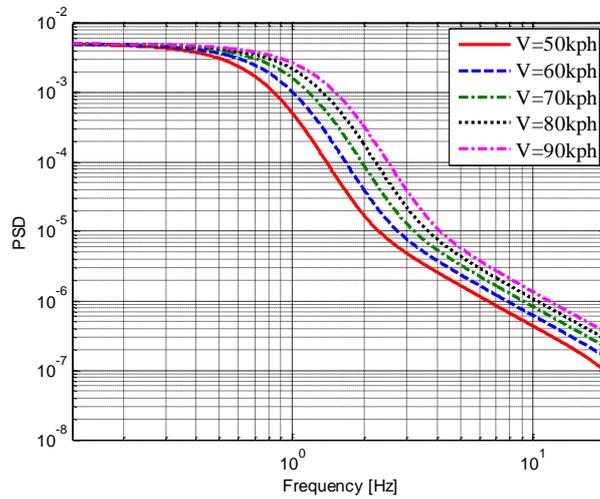

Fig. 6 Power spectral densities of random displacement inputs at different forward speeds
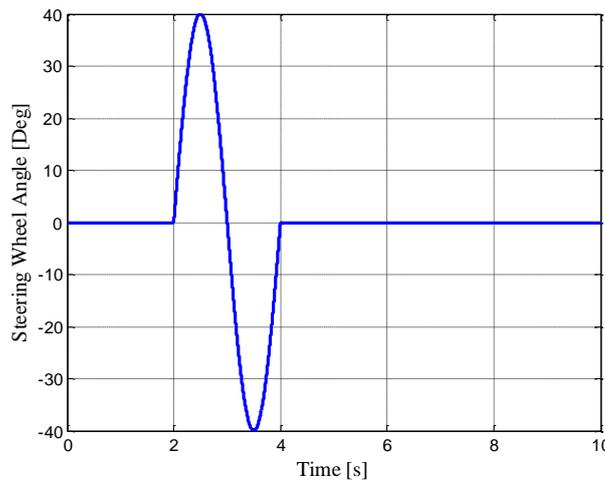

Fig. 7 Steering wheel input for lane change manoeuvre

Table 2 Vehicle and suspension parameters

| Parameter Definition	Symbol and Unit	Value
Piston Area	A_p (m^2)	0.007
Polytropic Gas Constant	κ	1.4
Front Left and Right Initial Gas Volumes	V_{30FL}, V_{30FR}, (L)	1.9
Intermediate Left and Right Initial Gas Volumes	V_{30ML}, V_{30MR}, (L)	1.9
Rear Left and Right Initial Gas Volumes	V_{30RL}, V_{30RR}, (L)	1.9
Front Left and Right Initial Gas Pressures	P_{30FL}, P_{30FR}, (bar)	23.7
Intermediate Left and Right Initial Gas Pressures	P_{30ML}, P_{30MR}, (bar)	21.9
Rear Left and Right Initial Gas Pressures	P_{30RL}, P_{30RR}, (bar)	20.6
Hydraulic Conductor Resistance	R_{4FL1RR}, R_{4FR1RL} (m^3/Pa.s)	2.92e-8
Hydraulic Conductor Resistance	R_{4ML1FR}, R_{4MR1FL} (m^3/Pa.s)	5.08e-8
Hydraulic Conductor Resistance	R_{4RL1MR}, R_{4RR1ML} (m^3/Pa.s)	5.85e-8
Oil Density	ρ (kg/m^3)	800
Orifice Damping Loss Factor	C_D	0.8
Vehicle Sprung Mass	M (kg)	9000
Distance Between Front Axle and Center of Gravity	a (m)	2.0
Distance Between Intermediate Axle and Center of Gravity	b (m)	0.3
Distance Between Rear Axle and Center of Gravity	c (m)	2.0
Front, Intermediate, and Rear Track Width	t_f, t_m, t_r (m)	2.0
Tire Mass	M_t (kg)	150
Tire Stiffness	k_t (N/m)	6e5
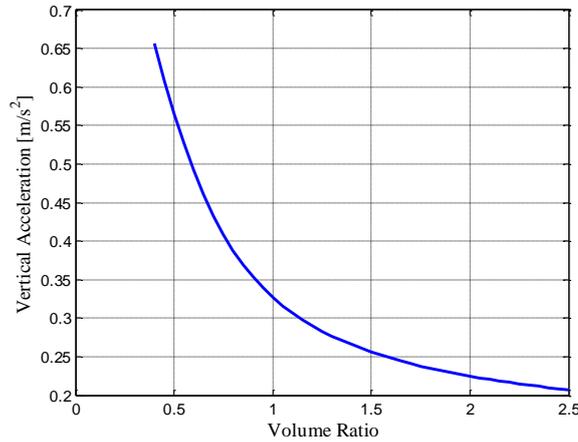
Fig. 8 rms of vertical acceleration

3.1 Parametric study

The parameters of the suspensions and vehicle used in the simulations are given in Table 2. Since the suspension has a nonlinear stiffness and damping characteristics, it does not have a
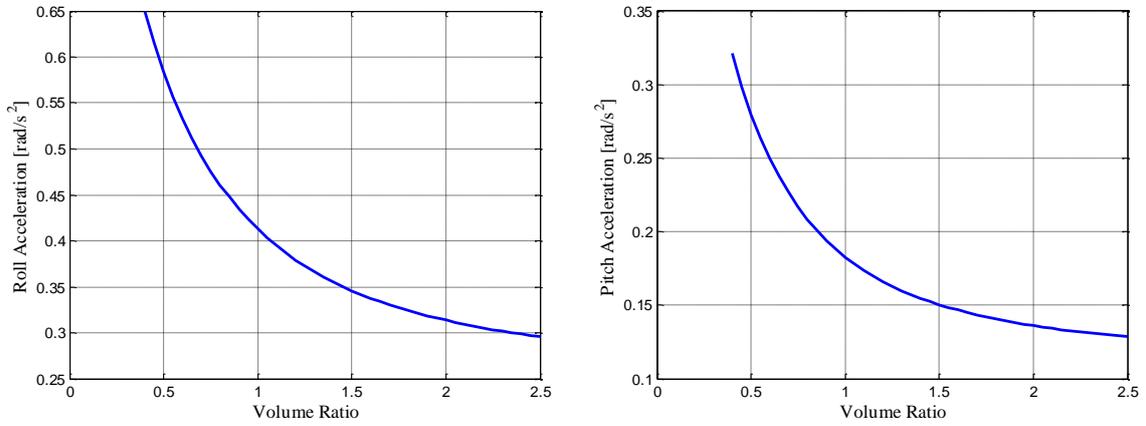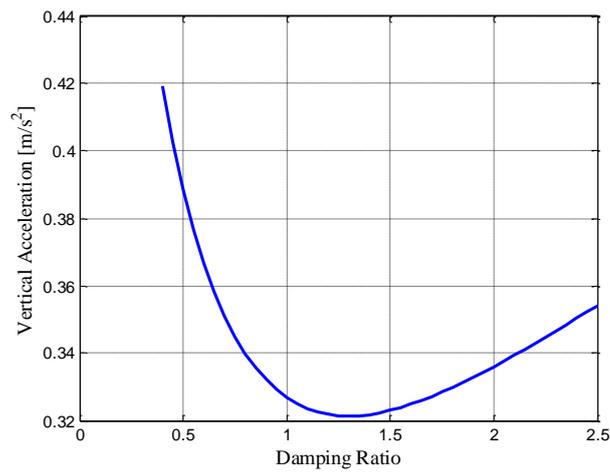
Fig. 9 rms of roll and pitch acceleration

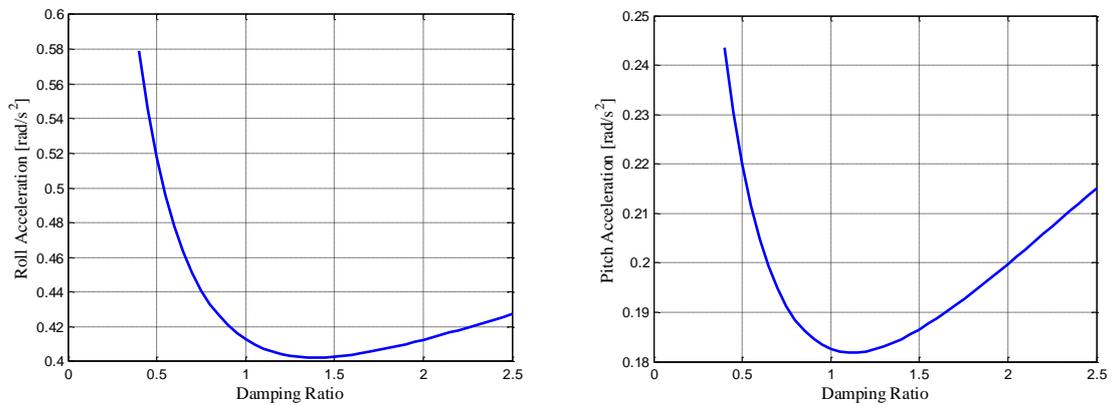Fig. 10 rms of vertical acceleration

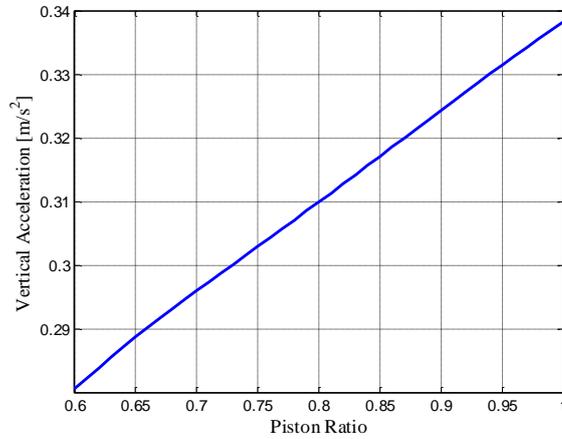Fig. 11 rms of roll and pitch acceleration
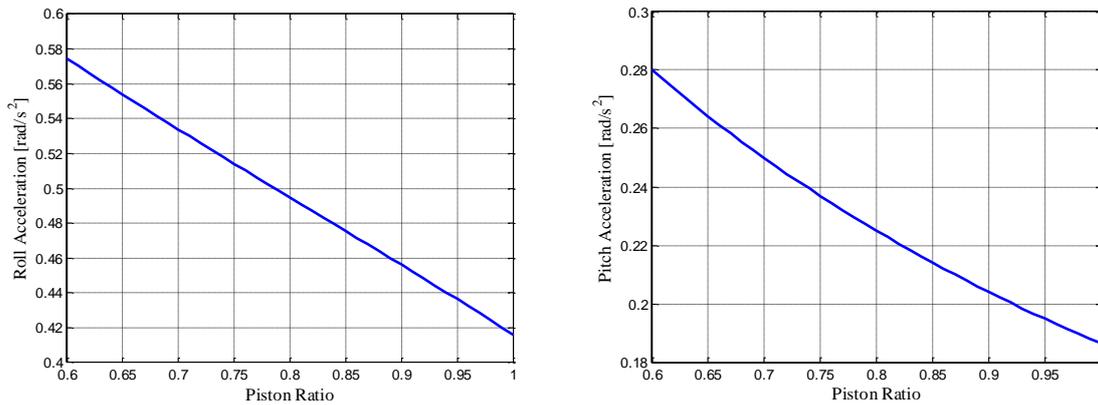
Fig. 12 rms of vertical acceleration

Fig. 13 rms of roll and pitch acceleration

constant stiffness and damping coefficients. Details of the nonlinear stiffness and damping characteristics of the suspension are defined in the study of Saglam (2016). The variations of the vertical, roll, and pitch accelerations with the gas volume ratio are presented in Figs. 8 and 9. As can be seen from results, when the gas volume ratio is lower, suspension stiffness increases and thus vertical, roll, and pitch accelerations also increase. This causes a degraded ride comfort performance.

The variation of the vertical, roll, and pitch accelerations with the damping ratio are given in Figs. 10 and 11. As can be seen from results, there is a certain damping ratio resulting in minimum acceleration in each case.

Finally, the effect of the piston ratio on the vertical, roll, and pitch accelerations are examined and the results are presented in Figs. 12 and 13. Piston ratio affects both the stiffness and the damping characteristics. With regard to stiffness, when the piston ratio is reduced, the vertical stiffness decreases; yet a tendency of increasing the pitch and the roll stiffness appear. With regard to damping characteristics, when the piston ratio decreases, vertical damping is reduced, and there is again a tendency to increased pitch and the roll damping. Therefore, increasing piston ratio
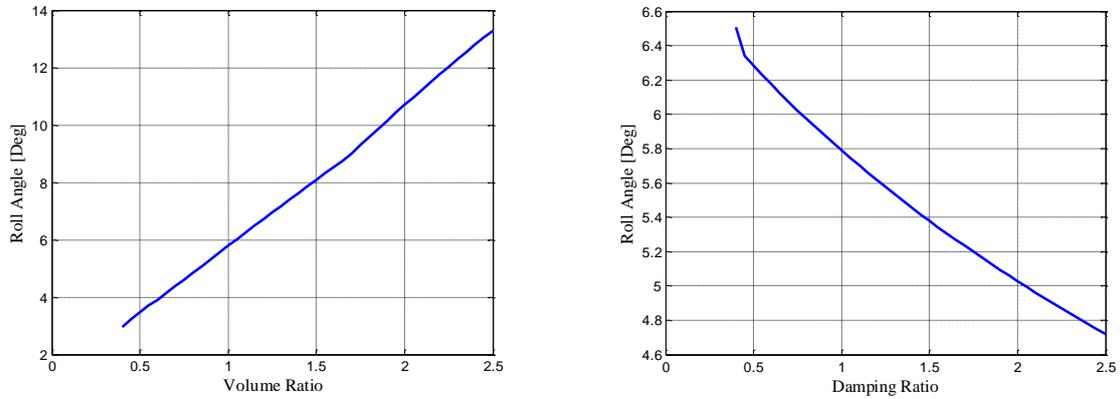
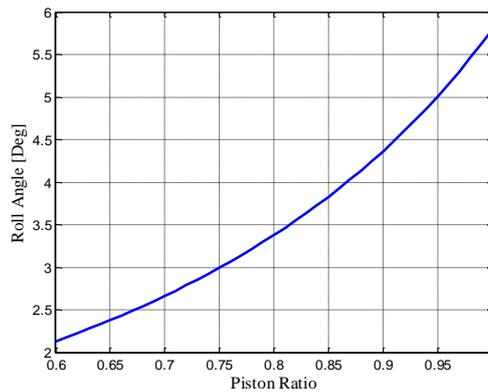Fig. 14 roll angle vs. volume and damping ratio

Fig. 15 roll angle vs. piston ratio

results in lower vertical ride comfort performance, and higher roll and pitch ride comfort performances.

Simulations are then performed with the lane change manoeuvre. Simulation results are shown in Figs. 14 and 15. The results show that, when the volume ratio is reduced the suspension stiffness increases, and the roll angle is reduced. When the damping ratio increases, maximum value of the roll angle decreases. The volume ratio has a stronger influence on the roll angle response than the damping ratio. When the piston ratio decreases, the roll stiffness increases, and the roll angle gets smaller.

In summary, as expected, making the suspension stiffer by reducing the gas volumes improves the vehicle handling, but degrades the vehicle ride comfort. When the piston ratio is decreased, vertical stiffness and damping are also decreased, yet roll stiffness and damping are increased. Therefore, there is a tendency of increasing ride comfort and vehicle handling performance simultaneously.

3.2 Optimization results

Table 3 Genetic algorithm parameters

Parameter	Value
Elite Count	2
Crossover Fraction	0.8
Pareto Fraction	0.35
Migration Interval	20
Migration Fraction	0.2

Table 4 Optimization results

	Ride Comfort (ϕ=8 Deg)			Handling (ϕ=4 Deg)		
	Uncon.	Intercon.	%	Uncon.	Intercon.	%
Acceleration (m/s^2)	0.90	0.43	55	1.32	0.48	62
Roll Angle (^{o})	7.9	4.4	35	4.0	4.0	0

Table 5 Optimum parameter sets

	Ride Comfort (ϕ=8 Deg)		Handling (ϕ=4 Deg)	
	Uncon.	Intercon.	Uncon.	Intercon.
Volume Ratio	1.47	2.50	0.76	2.26
Damping Ratio	0.83	0.40	1.73	0.50
Piston Area Ratio	-	0.60	-	0.60

After the effects of the design parameters on the accelerations and roll angle are examined, the optimization is performed. Both design parameters of the unconnected and interconnected HP suspension system are optimized. In this study, volume ratio, damping ratio, and the piston rod area ratio are taken identical for front, intermediate, and the rear suspension. Optimization is performed firstly for vehicle ride comfort and then for vehicle handling. For ride comfort optimization, the maximum roll angle is specified as 8 degrees, and for the handling optimization maximum roll angle is specified as 4 degrees for the lane change manoeuvre at the specified forward speed. For the optimization, a heuristics global optimization algorithm, genetic algorithm method (The Mathworks Inc. 2013, Chong and Zak 2008) is used. The parameters of the genetic algorithm are given in Table 3. The optimization results are given in Table 4, and the optimum parameter sets are given in Table 5.

Table 5 shows that the vehicle with the unconnected HP suspension system has a volume ratio of 1.47 and a damping ratio of 0.83 for the best ride comfort performance and in order to constrain the maximum roll angle to 8 degrees. For the vehicle with the interconnected HP suspension system, the volume ratio is set to the upper limit and the damping ratio is set to the lower limit in order to minimize the weighted vertical accelerations. However, the piston rod area is set to the possible minimum value for the roll angle constraint. Even though, 8 degrees roll angle constraint is imposed at the optimization, after optimization, 4.4 degree roll angle is obtained. When the optimization results for the unconnected and interconnected HP suspension systems are compared, it is observed that the vehicle with the interconnected HP suspension system has lower vertical acceleration than that of the vehicle with the unconnected suspension system. The vehicle with the interconnected HP suspension system has a lower maximum roll angle as compared with the

Table 6 Optimization results

	Ride Comfort (ϕ=8 Deg)			Handling (ϕ=4 Deg)		
	Uncon.	Intercon.	%	Uncon.	Intercon.	%
Acceleration (m/s^2)	0.77	0.46	40	1.00	0.48	52
Roll Angle (Deg)	7.7	5.0	35	4.0	3.9	3

Table 7 Optimum parameter sets for ride comfort optimization

	Unconnected	Interconnected
Parameter	Value	Value
Front Volume Ratio	1.00	2.45
Front Damping Ratio	1.61	0.76
Front Piston Rod Ratio	-	0.63
Intermediate Volume Ratio	1.47	2.45
Intermediate Damping Ratio	0.41	0.43
Intermediate Piston Rod Ratio	-	0.62
Rear Volume Ratio	2.50	2.50
Rear Damping Ratio	0.42	0.41
Rear Piston Rod Ratio	-	0.63

Table 8 Optimum parameter sets for handling optimization

	Unconnected	Interconnected
Parameter	Value	Value
Front Volume Ratio	0.50	2.39
Front Damping Ratio	2.50	1.28
Front Piston Rod Ratio	-	0.65
Intermediate Volume Ratio	0.44	1.82
Intermediate Damping Ratio	0.77	0.41
Intermediate Piston Rod Ratio	-	0.61
Rear Volume Ratio	2.50	2.47
Rear Damping Ratio	0.41	0.50
Rear Piston Rod Ratio	-	0.60

maximum roll angle of the vehicle with the unconnected suspension system.

For the improved handling behaviour of the vehicle, 4 degrees roll angle constraint is imposed during the optimization. As Table 5 illustrates, the vehicle with the interconnected HP suspension system has a somewhat higher volume ratio and lower damping ratio. These parameters result from the need to lower the vertical acceleration and thus increasing the ride comfort. However, the piston rod area is again set to its lower limit in order to reduce the roll angle. For the vehicle with the unconnected HP suspension system, a low value of the volume ratio and a high value of the damping ratio are obtained in order to limit the roll angle to 4 degrees. Thus, the suspension stiffness is increased, and thus ride comfort is degraded. Since the vehicle with the interconnected

HP suspension system has lower acceleration, it has better ride comfort performance. In order to reduce the roll angle and improve the handling performance, roll stiffness and damping should be increased. For a vehicle with the unconnected suspension system, the only way of achieving high roll stiffness and damping is to reduce the gas volume and increase the suspension damping. While increasing the roll stiffness and damping, vertical stiffness and damping are also increased and thus ride comfort is deteriorated. However, for a vehicle with the interconnected HP suspension system, the roll stiffness and damping can be increased either by reducing gas volumes, increasing the suspension damping, or by reducing the piston rod area. In the first case, both roll and vertical stiffness as well as damping are increased. However, in the second case, vertical stiffness and damping characteristics can be kept constant, while increasing pitch stiffness and damping. As a result, more than 50% improvement in ride comfort is obtained with equal handling performance by using the interconnected HP suspension system.

The same optimization procedure is also repeated with independent front, intermediate, and rear suspension parameters and the results in Table 6 to Table 8 are obtained.

As can be seen from Table 6, both unconnected and interconnected suspensions improve the ride comfort and handling performances of the vehicle. Similar to the previous results, interconnected HP suspension system have better ride comfort performance than the unconnected suspension.

As Tables 7 and 8 illustrate, for minimized acceleration, optimized parameters for front, intermediate, and the rear suspension units are set to different values. For the unconnected HP suspension system to satisfy the roll angle constraint the initial gas volume of the front suspension unit is set to an intermediate value and initial gas volumes of the intermediate and the rear suspension units are set to somewhat higher values for ride comfort optimization. On the other hand, for the interconnected HP suspension system, roll angle constraint is satisfied by lower piston rod ratios for ride comfort optimization. By this way, initial gas volumes of front, intermediate, and the rear suspension units are optimized to their upper values for ride comfort performance.

For handling optimization, initial gas volumes of the front and intermediate suspension units are set to their lower limits in order to constrain the roll angle. However, initial gas volume of the rear suspension unit is set to its upper limit for reduced vertical acceleration. Interconnected HP suspension system minimizes the vertical acceleration by raising the initial gas volumes to their upper limits and lowering the damping ratios to their lower limits. Roll angle constraint is satisfied by piston rod ratios set to their lower limits for the interconnected HP suspension systems.

4. Conclusions

In this study, suspension design parameters of a three-axle vehicle with the unconnected and interconnected HP suspension configurations are optimized. The main aim of the optimization is to improve the ride comfort together with handling and driving safety. The optimized suspension parameters for the unconnected HP suspension system are taken as the gas volumes and the suspension damping. For the interconnected HP suspension system, the piston rod area is also included in the optimized suspension parameter set. In the optimization, normalized forms of the suspension design parameters are used. The objective function is formed as the weighted rms of the sum of the vertical accelerations at different locations on the vehicle, and the maximum roll angle is imposed as the optimization constraint. Upper and lower limits are set to the optimized

parameters in order to get a physically realizable parameter set. In the optimization, genetic algorithm is used. Optimization is performed for two different vehicle performance characteristics, first of which is the improved ride comfort, and the second is the improved vehicle handling, for both the unconnected and interconnected HP suspension systems.

According to the optimization results, the vehicle with the interconnected HP suspension system has better ride comfort and handling performances with respect to vehicle with the unconnected HP suspension system. For the unconnected HP suspension system, the roll angle is lowered by reducing gas volumes and by increasing the suspension damping, which degrades the ride comfort. However, for the interconnected HP suspension system, the roll angle can be reduced by reducing the piston rod area. Therefore, suspension stiffness and damping in the vertical direction do not have to be increased, so that ride comfort is not affected. As a result, vehicle with the interconnected HP suspension system provides an alternative solution to the inherent conflict between vehicle ride and handling characteristics improvement.

Note

This paper is revised and expanded version of a paper entitled "Optimization of ride comfort for a three-axle vehicle equipped with interconnected hydro-pneumatic suspension system" presented at OTEKON2016, 8. Automotive Technologies Congress, Bursa, 23-24 May, 2016.

References

Bauer, W. (2011), *Hydropneumatic Suspension Systems*, Springer, Heidelberg.

Cao, D. (2008), "Theoretical analyses of roll- and pitch-coupled hydro-pneumatic strut suspensions", Ph.D. Dissertation, Concordia University, Canada.

Chong, E.K.P. and Zak, S.H. (2008), *An Introduction to Optimization*, 3rd Edition, Wiley-Interscience.

Ding, F., Han, X., Luo, Z. and Zhang, N. (2012), "Modeling and characteristic analysis of tri-axle trucks with hydraulically interconnected suspensions", *Vehic. Syst. Dyn.: Int. J. Vehic. Mech. Mobil.*, **50**(12), 1877-1904.

Els, P.S. and Uys, P.E. (2003), "Investigation of the applicability of the dynamic-Q optimization algorithm to vehicle suspension design", *Math. Comput. Model.*, **37**(9-10), 1029-1046.

ISO, International Organization for Standarization (1977), *ISO 2631: Evaluation of Human Exposure to Whole-Body Vibration*.

Joo, F.R. (1991), "Dynamic analysis of a hydropneumatic suspension system", M.Sc. Dissertation, Concordia University, Canada.

Saglam, F. (2016), "Optimization of ride comfort for vehicles equipped with passive and active hydro-pneumatic suspensions", Ph.D. Dissertation, Middle East Technical University, Turkey.

Saglam, F. and Unlusoy, Y.S. (2014), "Modeling and state dependent riccati equation control of an active hydro-pneumatic suspension system", *Proceedings of the International Conference of Control, Dynamic Systems, and Robotics*, Ottawa, Canada, May.

Saglam, F. and Unlusoy, Y.S. (2016a), "Modelling and simulation of a three-axle vehicle with interconnected hydro-pneumatic suspension system", *Proceedings of the Fisita World Automotive Congress*, Busan, Korea, September.

Saglam, F. and Unlusoy, Y.S. (2016b), "Analysis of interconnected hydro-pneumatic suspension system for load sharing among heavy vehicle axles", *Proceedings of the 3rd International Conference on Control, Dynamic Systems, and Robotics*, Ottawa, Canada, May.

Smith, W.A., Zhang, N. and Hu, W. (2011), "Hydraulically interconnected vehicle suspension: Handling performance", *Vehic. Syst. Dyn.: Int. J. Vehic. Mech. Mobil.*, **49**(1-2), 87-106.

Smith, W.A., Zhang, N. and Jeyakumaran, J. (2010b), "Hydraulically interconnected vehicle suspension: Theoretical and experimental ride analysis", *Vehic. Syst. Dyn.: Int. J. Vehic. Mech. Mobil.*, **48**(1), 41-64.

The Mathworks Inc. (2013), *Matlab Global Optimization Toolbox, Genetic Algorithm*.

Thoresson, M.J. (2003), "Mathematical optimization of the suspension system of an off-road vehicle for ride comfort and handling", M.Sc. Dissertation, University of Pretoria, Pretoria, South Africa.

Thoresson, M.J., Uys, P.E. and Snyman, J.A. (2009), "Efficient optimization of a vehicle suspension system using a gradient-based approximation method, part 1: Mathematical modelling", *Math. Comput. Model.*, **50**(9-10), 1421-1436.

Thoresson, M.J., Uys, P.E. and Snyman, J.A. (2009), "Efficient optimization of a vehicle suspension system using a gradient-based approximation method, part 2: Optimization results", *Math. Comput. Model.*, **50**(9-10), 1437-1447.

Zhang, N., Smith, W.A. and Jeyakumaran, J. (2010a), "Hydraulically interconnected vehicle suspension: Background and modeling", *Vehic. Syst. Dyn.: Int. J. Vehic. Mech. Mobil.*, **48**(1), 17-40.

Zuo, L. and Nayfeh, S.A. (2003), "Low order continuous-time filters for approximation of the ISO-2631-1 human vibration sensitivity weightings", *J. Sound Vibr.*, **265**(2), 459-465.

FO